The Thesis Committee for Felicia Teri Konopka
Certifies that this is the approved version of the following thesis:

Synthesis of Organic Biaryl and Aryl Silyl Ether Linkers for Surface Functionalization of Silicon Semiconductors

APPROVED BY
SUPERVISING COMMITTEE:

Supervisor:

Michael J. Rose

Emily L. Que

Synthesis of Organic Biaryl and Aryl Silyl Ether Linkers for Surface Functionalization of Silicon Semiconductors

by

Felicia Teri Konopka, B.A.; M.S.; M.S.

Thesis

Presented to the Faculty of the Graduate School of

The University of Texas at Austin

in Partial Fulfillment

of the Requirements

for the Degree of

Master of Arts

The University of Texas at Austin

May 2017

Abstract

Synthesis of Organic Biaryl and Aryl Silyl Ether Linkers for Surface Functionalization of Silicon Semiconductors

Felicia Teri Konopka, M.A.

The University of Texas at Austin, 2017

Supervisor: Michael J. Rose

Abstract: Functional organic materials for use in inorganic semiconductor applications is of high scientific interest due to the need for flexible, conductive materials that can be utilized in solar energy applications. Herein is described a synthetic route for a new variant of biphenylene linker called **2Ldm-OTf-bpA**, which can be used as a building block for future conductive oligophenylene materials in semiconductor devices. With unique *ortho*-functionalized dimethoxy handles and para-functionalization via triflate and bromo groups, this linker can be chemically modified at the bromo position to attach to silicon semiconductor surfaces. Additionally, a synthetic route for **1-LdSihex$_3$-OTf** is presented which utilizes the modular synthon **1Ld-OH-OTf** that can be synthetically modified to generate many variations of small molecules, which can be used to control the steric spacing of molecules on surfaces during functionalization. Conversely, the

triflate group can be utilized as a synthetic modification point for future studies of molecular wire growth on silicon surfaces.

These molecular wires will be the foundation of future studies for developing a hybrid molecular/materials (HMM) layer on Si(111). These surfaces can then act as anchor points for catalysts for the production of solar fuels conversion such as H_2 from water or the reduction of CO_2 to methanol.

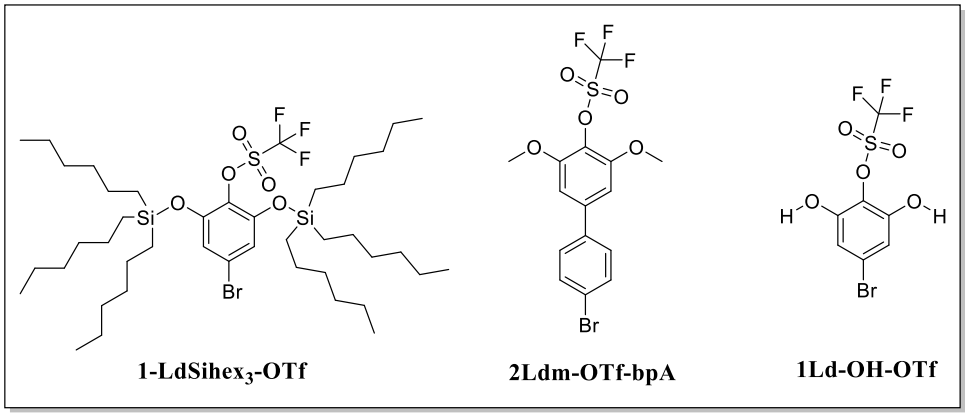

Table of Contents

List of Figures vii

INTRODUCTION.....1

***Molecular Wires in Molecular Electronics*.....1**

***Electron Transfer via Molecular Wires* 1**

***Future Applications of Functionalized Oligophenylene Molecular Wires*……3**

***Designing Conductive Oligophenylene Moleular Wires* 3**

***Materials for Semiconductor Devices* 6**

***Inorganic Semiconductor Materials* 7**

***Organic Semiconductor Materials*……12**

RESULTS AND DISCUSSION 15

CONCLUSION 22

EXPERIMENTAL PROCEDURES 23

***Appendix A Supplementary Information* 33**

***References* 47**

List of Figures

Figure 1: 4'-bromo-3,5-dimethoxy-[1,1'-biphenyl]-4-yl trifluoromethanesulfonate (2Ldm-OTf-bpA)……..……..5

Figure 2: 4-Bromo-2,6-bis((trihexylsilyl)oxy)phenyl trifluoromethanesulfonate (1LdSihex$_3$-OTf)…….....5

Figure 3: Classes of Semiconductor Materials…….....6

Figure 4: Energy Bands in Materials at 0 K…….....9

Figure 5: Structural Representations of Silicon…….....10

Figure 6: Molecular Orbital Diagram of sp^3 Tetrahedral Site…….....10

Figure 7: Diagram of an infinite sp^3 Td Molecular Orbitals……..….....11

Figure 8: HOMO/LUMO in a Diatomic and DOS Diagram……..…….....12

Figure 9: A Few Examples of Semiconductor Materials……..…….....13

Figure 10: Suzuki Cross-Coupling Catalytic Cycle……..…….....18

Introduction

Molecular Wires in Molecular Electronics

Kirczenow et al. define[1] molecular wires as "a single molecule that forms an electrically conducting bridge between a pair of metal contacts." Due to the growing field of molecular electronics[2], there is high interest in synthesizing novel organic molecular wires for specific semiconductor applications within the world of nanoscale technology. These molecular electronic applications range from power devices such as diodes, current rectifiers in circuits and devices or transistors for switches or amplifiers in memory and digital logic applications.[3] Photonic devices that harness energy from light include but are not limited to LEDs, lasers, and solar cells, while sensor devices are function specific and drive many biometric applications.[4]

Electron Transfer via Molecular Wires

In order to design a device for any of the above applications, it is critical to harness the structural and electronic properties of synthetic organic molecules for electron transfer. Numerous studies have shown that when placed between two electrodes, molecular bridges or wires of varying length, composition, torsion angle, and donor/acceptor abilities are conductive and can have effective electron transfer.[5]

Inspired by this knowledge, we were interested in utilizing a functionally-designed synthetic organic molecular wire that could contribute structural and electronic properties that would facilitate electron transfer through a photodiode metal-insulator-semiconductor (MIS)[6] device for eventual application for solar fuels conversions.

The idea that a molecular wire could be designed to conduct current in the forward direction as a molecular rectifier is a concept pioneered by Aviram and Ratner.[7] The AR diode consists of pi-donor (πD) and pi acceptor (πA) fragments spaced by a σ or π molecular bridge to form a D-σ-A or D-π-A. However, amongst the existing conducting donor-acceptor systems, one would notice that not all systems contain a distinct or discrete σ or π molecular bridge. For this reason, Aviram and Ratner concluded that the energy levels of the highest occupied molecular orbital (HOMO) of the πD and lowest occupied molecular orbital (LUMO) of the πA relative to the Fermi level of the electrodes have the most dominating effect on conductivity. This is in contrast to the Ellenbogen and Love (EL) theory[8] that states fluctuations in the molecular donor-acceptor HOMO/LUMO gap result from electronic changes solely within the molecule. The concept of the AR diode offers theoretical support for experiments that have shown that for a given molecular wire, effective electron transfer is not necessary dependent on conjugation or symmetry. For instance, Tao, et. al. studied bipyrimidinyl-biphenyl and tetraphenyl diblock pn junction molecules of asymmetric and symmetric orientation between two electrodes and found that despite asymmetry and incomplete conjugation, under applied bias, the bipyrimidinyl-biphenyl diblock molecular wire facilitated electron transfer better than the symmetric tetraphenyl diblock molecule and

acted like a D-σ-A structure as a result of rectification.[9] In addition to rectifying molecular wires, conductive rigid molecular wires are also common in the form of conjugated carbon chains of phenyl or unsaturated hydrocarbons.[10]

Future Applications of Functionalized Oligophenylene Molecular Wires

In addition to understanding electron transfer through molecular wires, we are also interested in incorporating them into a solid-state device that can maintain or improve electron transfer during catalysis[12] in the presence of a passivating, insulating metal oxide. Collectively, this hybrid molecular materials (HMM) device contains conducting, covalently bound molecular wires to facilitate electron transfer within a transparent metal oxide insulator to protect the molecular wire and Si(111) electrode. Comparatively, understanding electron transfer through this semiconductor-insulator-metal electrode system in the presence and absence of molecular wires will offer insight into the rate of electron transfer within this device.

Designing Conductive Oligophenylene Molecular Wires

Specifically, molecular wires that contain functionality that allows for post-synthetic modification is valuable, so that the molecular wire can have maximum utility in the system of interest. Aromatic molecular wires like oligophenylene wires are of

interest because these conductive molecular wires are more rigid and therefore can be used to spatially control and modify a given silicon semiconductor surface with available atop functionalization sites (ex: Si(111)).[10]

With this knowledge in mind, we were able to fashion a molecular wire suitable for function and not limited by its inherent symmetry and conjugation. Our design utilizes ortho-substituted oligophenylene monomer units cross-coupled to phenyl monomers for wire growth in an alternating pattern. The ortho-substitution of the oligophenylene wires utilizes dimethoxy substituents that allow for device functionality by serving as built-in anchors for covalent modifications. These compounds can be deprotected to alcohol groups and functionalized to surface steric spacer linkers, or used to interact directly with an insulating metal oxide layer.[11]

Synthesizing molecular wires that are designed to serve a specific function can be difficult. This is largely due to the challenges of designing efficient organic methodology, while mitigating the reactivity and cost of the starting material or intermediate.[12] From a practical standpoint, good methodology also heavily relies on a synthetic scheme that requires the fewest steps and starts from low cost starting materials.

Herein is described the synthesis of a novel biaryl molecular wire **2Ldm-tf-bpA** and **1-LdSihex$_3$-tf** using optimum methodology. The synthon **2Ldm-tf-bpA** contains *ortho*-dimethoxy (-OMe) substituents and *para*-functionalized substituents of triflate (-OTf) and bromo (-Br) (Figure 1).

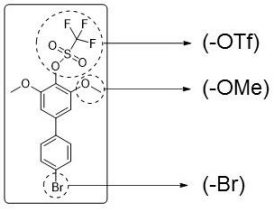

Figure 1: 4'-bromo-3,5-dimethoxy-[1,1'-biphenyl]-4-yl trifluoromethane sulfonate **(2Ldm-OTf-bpA)** and relevant functionalities

Additionally, the synthesis of **1-LdSihex$_3$-tf** (Figure 2), which contains *ortho*-silyl (-OSi(hex)$_3$) substituents with triflate (-OTf) and bromo (-Br) functionalities is described.

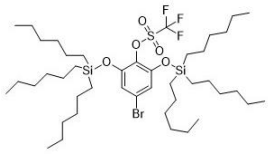

Figure 2: 4-bromo-2,6-bis((trihexylsilyl)oxy)phenyl trifluoromethanesulfonate **(1LdSihex$_3$-OTf)**

Ortho-dimethoxy groups were selected to allow for deprotection of the methoxy groups to hydroxyl groups (-OH), which can be post-synthetically modified with a countless array of new functionalities. Additionally, the dimethoxy groups aid in selectivity in Suzuki carbon-carbon (C-C) cross-coupling reactions.[13] Differential

installment of coupling leaving groups allows for selective cross-coupling reactions for possible modifications of a given molecular wire.

Materials for Semiconductor Devices

In order to design a semiconductor device for any given application, its components must contain a material that will facilitate the flow of electrons through the device. Broadly speaking, a conductive substrate is any material that allows a current of electricity (or flow of electrons) to pass through it.[15] A conducting material is one in which the atoms have valence electrons that are loosely bound and mobile. When these electrons repel each other they gain potential energy. This collective event results in the conductivity of a metal such as copper. Semiconducting materials are partially conductive materials and can be of inorganic or organic composition (Figure 3). Inorganic semiconductors are often crystalline solids like germanium or silicon.[16] Organic semiconductors can be small molecules, oligomers or polymers.[17]

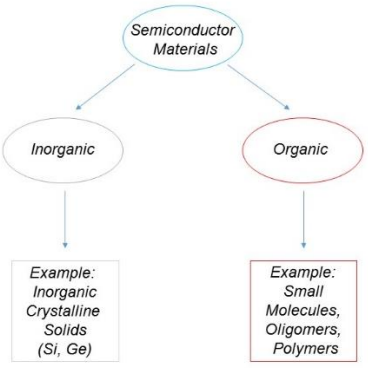

Figure 3: Classes of Semiconductor Materials

Inorganic Semiconductor Materials

Within intrinsic crystalline inorganic semiconductors (which are the compositionally the purest form of semiconductors) a small amount of applied thermal excitement results in movement between the silicon atoms or lattice vibrations. Due to this movement, one electron leaves its position in the silicon atom, leaving behind a hole or vacancy in the silicon atom and the overall semiconductor lattice. The motion of this electron along with other excited electrons in the lattice results in a current or electronic conduction.[16]

The number of electrons available for conduction will depend on: a) the arrangement of electron states or levels with respect to energy; and b) the way these states are occupied by electrons. These variables can be derived by the properties of the atomic energy levels of a single atom of a given solid. For instance, for silicon, the valence shell configuration is $[Ne]3s^2 3p^2$. It is expected that the outermost valence electron shells 3s and 3p will have the most splitting since they are easiest to perturb. The lower energy band representative of the sum of 3s orbitals of each Si atom will contain N (one energy state per each atom of silicon in the solid) electron energy states. The higher energy band representative of the sum of 3p orbitals of each Si atom will contain 3N (three energy states per each atom of silicon in the solid) electron energy states. This is related to the atomic principle energy level with respect to orbital angular momentum in a particular valence shell. For instance, for 3p, the orbital angular momentum is $l = 1$, meaning that there are three possibilities for the orientation of the

orbitals or m_l = (-1, 0, 1). So analogously in a solid, this is why 3N electron energy states exist.[16]

In a solid, with N atoms, the atomic states of each atom will be split into closely spaced electronic states (due to electron and nuclei repulsion of adjacent atoms). These electronic energy states then collectively form an energy band and the respective electric properties of a given solid. When these electron energy levels are then filled with electrons, different band structures may result. At 0 K, there are four possible band structures due to different possible ways of occupying the bands. The first possibility is where the outermost band is partially filled with electrons. At 0 K, this structure is common for copper in the diamagnetic state. The second possibility is where an empty band and filled band overlap. At 0 K, this structure is common for magnesium in the paramagnetic state. For these two possibilities, the highest filled state is called the Fermi level energy (E_F). To excite an electron it must be promoted to an energy above the E_F. In the case of copper or magnesium, very little energy is needed to cause this promotion.[16]

Lastly, the two other possibilities that exist are when one fully occupied band known as the valence band (VB) is separated from an empty conduction band (CB) with an energy "band gap" between them. When the energy band gap is large (> 4 eV), an insulator material results. When the energy band gap is small (< 4 eV), a semiconductor material results (Figure 4). In these materials an electron must have the energy equal or greater to the band gap of the material in order to be promoted to the conduction band. This excitation can be caused by heat or light.[16]

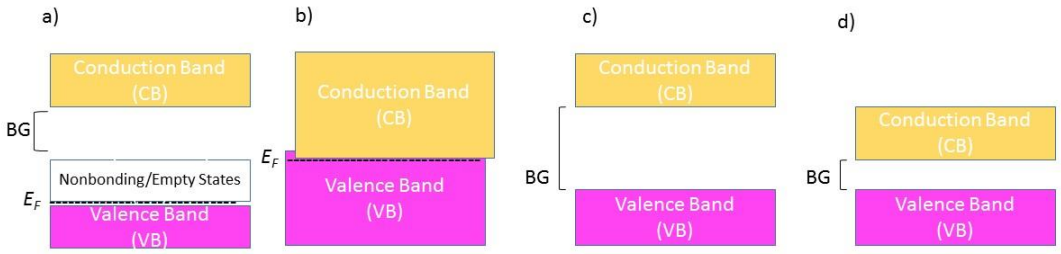

Figure 4: Energy Bands in Materials at 0 K.[16] a) Diamagnetic Solid (ex: Cu) b) Paramagnetic Solid (ex: Mg) c) Insulator d) Semiconductor

BG=Band Gap, E_F=Fermi Level Energy.

The concept of a valence band and conduction bands applied to solids and materials is heavily derived from the fundamental ideas of molecular orbital theory applied to inorganic or organic molecules. In fact, one can argue that when you go from a small set number of molecular orbitals for a molecule to a solid in which there is a very large number of orbitals, you essentially need molecular orbital theory applied to a very large molecule—in this case a solid.[18]

To understand how this could be possible, one can start with inorganic crystalline solid silicon. It is a diamond cubic unit cell with two primitive cells with two tetrahedral Si_4 clusters each (Figure 5).[16]

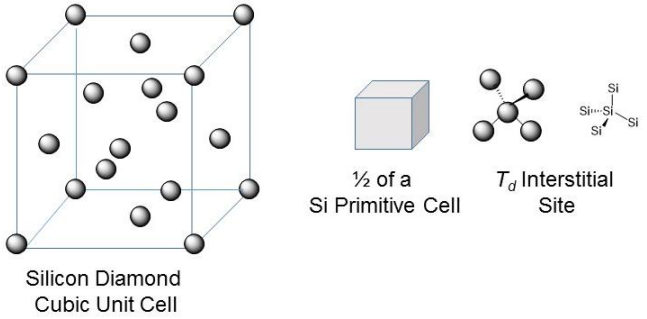

Figure 5: Structural Representations of: a) Silicon Unit Cell b) Half of a Silicon Primitive Cell c) Local T_d Geometry within Unit Cell

A MO diagram for single tetrahedral (T_d) sp^3 silicon molecule can be constructed (Figure 6).

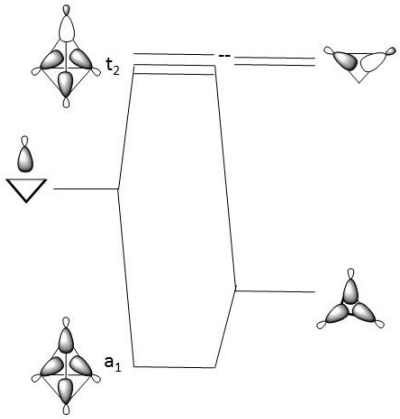

Figure 6: Molecular Orbital Diagram[18] of sp^3 Tetrahedral Site

One could then apply this to a chain of silicon sp^3 hybridized clusters, where all orbitals of each silicon T_d would be the same, but as the number of the same orbital of a given energy increases, these orbitals begin to converge and become a band (Figure 7).

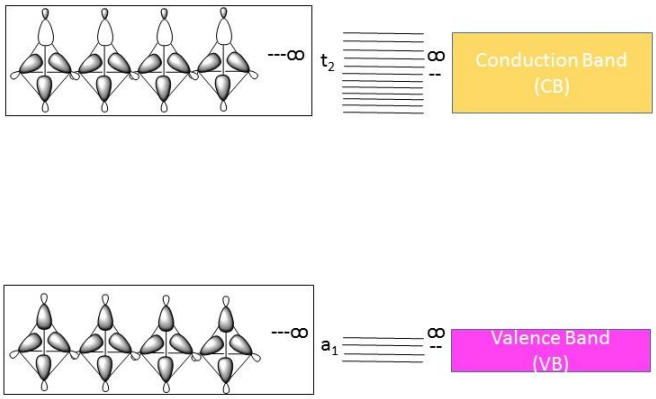

Figure 7: Diagram of an infinite sp^3 T_d Molecular Orbitals Converging to Bands[18]

Since in a solid like silicon, electrons are moving in a 3D lattice and not a straight chain, advanced applications of molecular orbital theory can account for this by taking the silicon straight chain and imagining it to be a ring, by simply tying the ends together as a cyclic molecule. This ensures a continuous "sea of electrons". [18]

The interesting feature of bands is that the bottom of the valence band represents bonding throughout and receives maximum stabilization. The most antibonding character is found at the top of the band, where in the middle there are the nonbonding orbitals. This trend follows that of the ordering of molecular orbitals in the MO diagrams for Li_2 to N_2. Additionally, in the same way that we would populate a molecular orbital with one or two electrons, bands can be populated with electrons and this is represented as density of states diagrams in solids, which are rotated Gaussian curves at different energy levels, representing the probability of finding an electron in that particular energy region. The highest energy electrons in a valence band are at the top part of the band, where the population can be described with its density of states. This idea is directly

analogous to the HOMO in a molecular orbital diagram of a single molecule, whereas the lowest energy orbitals in the conduction band are analogous to the LUMO in a MO diagram of a single molecule (Figure 8).

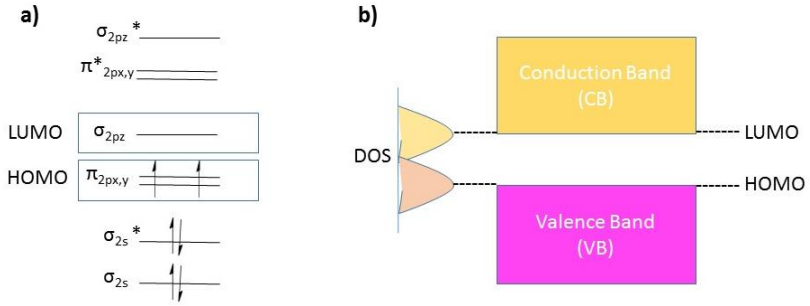

Figure 8: a) The HOMO/LUMO in a diatomic (B2 shown) molecule b) The HOMO/LUMO in a representative solid with Density of States (DOS) diagrams

Organic Semiconductor Materials

In addition to inorganic semiconductors, organic semiconductors also exist. Typically they are small molecules and oligomers or polymers. Some varieties of organic oligomer molecular wires are shown in Figure 9. These materials [19] are designed to facilitate charge transport and will preferentially transport either holes or electrons. It is also generally accepted that the ability of a material to transport charges is relative to the ease of charge injection from the electrode. When the Fermi level (or probability of

finding an electron) of the organic material matches that of the electrode, charge transfer will be facilitated.

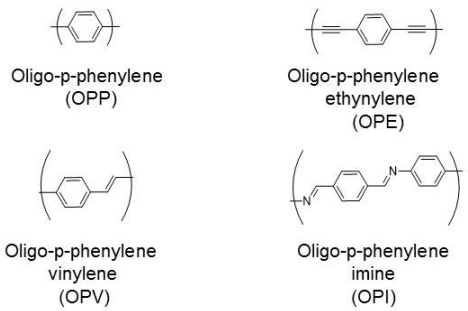

Figure 9: A Few Examples of Semiconductor Materials

For instance, for a material like n-type silicon, with a slight excess of negative carriers or electrons relative to the silicon material, its Fermi level would be expressed as the probability of its highest energy valence band electrons being close to the empty conduction bands of the electron poor (or electron accepting) organic molecule. In that case, the organic material would be an electron acceptor where its Fermi level represents the probability of it accepting an electron (or its electron affinity). A similar situation can be envisioned where the material is hole-rich (instead of electron rich). In that case, the organic material should be electron rich or donating, so expressing its Fermi level in terms of ionization potential (willingness to give up electrons) would be important to match to the Fermi level of the corresponding material.[19]

Organic semiconductors are often characterized as n- or p- type materials and with respect to the electrode of interest. In an inert system (ex: where an organic semiconducting material lies between two gold electrodes), these materials are classified

relative to their intrinsic properties in the absence of any external perturbation. For instance, n-type materials are donor materials because they are electron rich and p-type materials are acceptor materials because they are electron poor. With respect to a semiconductor electrode system, these materials are classified with respect to the semiconducting material that they would complement, not relative to their intrinsic properties. For instance, an electron rich organic material would be a good hole transporter for a hole-rich p-type material, therefore an electron rich material would be classified as a p-type material because it is a good hole transporter. Conversely, an n-type organic semiconductor material would be electron poor and a good electron transporter for an electron rich material.[19]

Below, we describe the synthesis of a novel biaryl molecular wire **2Ldm-OTf-bpA** and aryl silyl ether **1-LdSihex$_3$-OTf**, both of which could be post-synthetically fashioned as either a n- or p-type material and applied for use in hybrid molecular/materials (HMM) on Si(111) surfaces for the production of solar fuels.

RESULTS AND DISCUSSION

In order to successfully synthesize 4-bromo-2,6-bis((trihexylsilyl)oxy)phenyl trifluoromethanesulfonate **(1LdmSihex$_3$-OTf)** and 4'-bromo-3,5-dimethoxy-[1,1'-biphenyl]-4-yl trifluoromethanesulfonate **(2Ldm-OTf-bpA)**, the following intermediates were synthesized (Scheme 1).

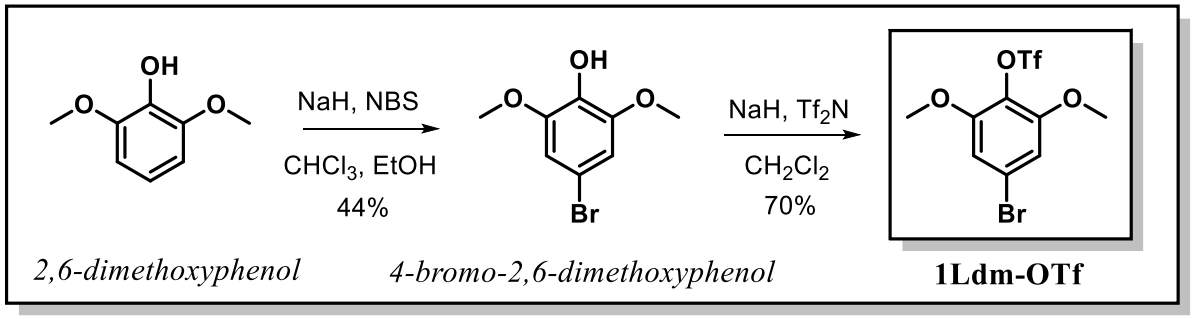

Scheme 1

Bromination of the para-position of 2,6-dimethoxyphenol with N-Bromosuccinamide (NBS) yields the product 4-bromo-2,6-dimethoxyphenol. However, one challenge with this product is that it must be isolated from the unavoidable meta-substituted bromo products (resulting from directing effects of the other substituents), which can be separated via column chromatography with extreme diligence and/or multiple columns. Since 4-bromo-2,6-dimethoxyphenol is the first step in a multi-step synthesis, attempts to optimize the yield involved various recrystallization and reported literature procedures[20]. Moderate success was identified for crude product recrystallization from $CHCl_3$/hexanes

or diethyl ether. However, this was dependent on recrystallizing from a large batch of crude material (≥ 10 g) and resulted in significantly diminished yields (~10-20%) with trace impurities (~2-5%) still present. The subsequent step of converting the –OH to –OTf was attempted with recrystallized material, however the purification of **1Ldm-OTf** produced by this method was significantly more difficult to purify (with drastically reduced yields) compared to **1Ldm-OTf** produced by 4-bromo-2,6-dimethoxyphenol that had been column purified. Since these products are intended for use in future semiconductor applications, synthetic routes leading to the purest grade materials were selected. Therefore, column chromatography of crude 4-bromo-2,6-dimethoxyphenol as reported in the supporting information was utilized and identified as the best optimized synthetic procedure with a yield of 44% pure product.

Following the isolation of pure bromo-2,6-dimethoxyphenol, conversion to **1Ldm-OTf** proceeds smoothly in high yields (70%) with NaH and *N*-phenyl-bis(trifluoromethane) sulfonamide. Next, in order to convert **1Ldm-OTf** to **1LdmSihex$_3$-OTf** (Scheme 2), deprotection of the dimethoxy groups with BBr_3 was performed.

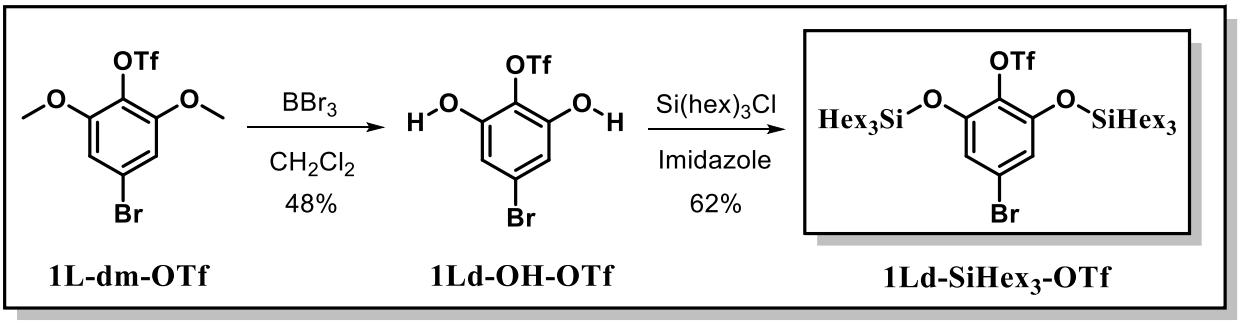

Scheme 2

While dimethoxy groups were utilized as robust protecting groups installed in a commercially available starting material, the deprotection procedure required significant optimization. It was found that the number of equivalents of BBr_3 and the time of the reaction had the most effect on the ratio of the products. Upon the first addition of 2.5 equivalents and after one day, the partial conversion to the mono-deprotected product results. A subsequent addition of 2.5 equivalents of BBr_3 after the second day results in full conversion to the mono-deprotected product, with a small amount of double-deprotected material. If more BBr_3 is added, after the second day, decomposition occurs and products intractable from the desired diol are obtained. In evaluating the literature, one finds that some studies show that the mechanism of BBr_3 deprotections are not always straightforward S_N2 reactions. For instance, Lord et. al. has proposed[21] that charged intermediates and bimolecular mechanisms may occur in the demethylation of aryl methyl ethers. Based on that premise, it was proposed that by performing two separate methyl ether deprotections (with isolation of the monodeprotected product), the doubly deprotected product could be isolated. That insight led to a successful modification of the procedure which evolved into the two-step deprotection process. In addition, given that charged intermediates may be a part of the deprotection, it was hypothesized that performing the reaction under dark conditions (covering flask in foil, to minimize possible degradation by radicals) would improve yields; this was found to be the case. Additionally, a modified work-up utilizing diethyl ether and sodium bicarbonate was found to be most successful in maximizing the yields. Other noteworthy observations in experiments designed to deprotect the dimethoxy groups

include that reaction of **1Ldm-OTf** is stable to 48% HBr at 150 ^{o}C and that **1Ldm-OTf** with LiCl in DMF at 150^{o}C reacting overnight results in efficient dimethoxy deprotection, but with loss of the triflate group.

After deprotection, **1Ld-OH-OTf** can be reacted with various reagents to install different ether derivatives. In particular, our interest was in the silyl ether groups (which have extensive precedent in semiconductor devices[22]), so **1Ld-OH-OTf** was reacted with chlorotrihexylsilane, imidazole and DMF to form **1Ld-Sihex$_3$-OTf**. Purification of **1Ld-Sihex$_3$-OTf** is required in order to separate the product from silylhexyl byproducts. It is important to note that **1Ld-OH-OTf** and **1Ld-Sihex$_3$-OTf** are not benchtop stable and will decompose within 4-8 hours if not stored properly in the absence of light and moisture, at low temperatures (< -20 ^{o}C), and under N_2 atmosphere.

Preparation of the molecular wire component **2Ldm-OTf-bpA** was performed via Suzuki cross-coupling of **1Ldm-OTf** with 4-bromophenyl boronic acid. Suzuki cross-coupling involves three main steps: oxidative addition, transmetallation, and reductive elimination (Figure 10).

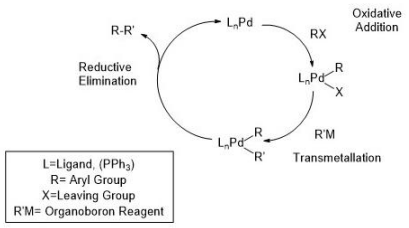

Figure 10: Suzuki Cross-Coupling Catalytic Cycle

In practice, many variations of Suzuki couplings exist depending on the substrate and catalyst employed. However, the general mechanism is that first the substrate (in this case **1Ldm-OTf**) acts as an electrophile as the palladium catalyst oxidatively inserts into the C-X bond. Then the resulting Pd^{II} metal complex undergoes nucleophilic attack during transmetallation. Finally, reductive elimination forms the desired product.[23] Among Suzuki cross coupling reactions, it is widely believed that the rate limiting step is the oxidative addition step.[24]

Since **1Ldm-OTf** functional groups of –OTf and –Br are relatively close in reactivity (due to their weaker bond dissociation energy, ~80-85 kcal/mol as compared to chlorine, ~96 kcal/mol), it is difficult to a priori predict where a Pd^0 catalyst would insert during oxidative addition based on bond dissociation energies.[25] During the oxidative addition step, it is plausible that C-OTf or C-Br insertion may occur. However, given that a C-OTf insertion by palladium would result in a highly sterically congested palladium center for the palladium (II) complex intermediate, likely this insertion is slower and favored at lower temperatures. Indeed this is the case, as reported by the literature. With Suzuki couplings, when in competition with –OTf, -Br displacement was observed regardless of whether the catalyst has chelating or monodentate ligands. It was also noted that the temperature of the reaction and solvent dictated whether or not C-Br insertion was the dominant or only product. Higher temperatures and toluene solvent were found to facilitate C-Br insertion only. If C-OTf insertion was desired, with Negishi and Stille coupling reactions, Pd^0 insertion occurs into the C-OTf bond with catalysts containing chelating diphosphine ligands (ex: $Cl_2Pd(dppp)$ is utilized). Another

noteworthy detail includes the nature of the salt[26] which facilitates the transmetallation step. If the palladium complex after oxidative addition is more stable, a stronger base would be required for the transmetallation step. Based on hard soft acid base concepts (HSAB) for this intermediate, the $(L)_3Pd^{II}$-Br complex would be hypothesized to be more stable, since a soft acid (Pd^{II})-soft base (Br^-) match compared to a $(L)_3Pd^{II}$-OTf complex which would be a less compatible match (i.e less stable compound) versus a soft acid (Pd^{II})-hard base (OTF^-) pair.

With that knowledge in hand, preparation of **2Ldm-OTf-bpA** was performed at high temperatures, in toluene, and with strong bases first (Na_2CO_3). While these conditions resulted in the formation of the product, crude mixtures always contained a trace amount (~1-5%) of unknown material (possibly polymeric) which was intractable from the desired product by column chromatography. For this reason, reaction conditions involved a solvent change to THF. With THF, product was initially observed in about a 30% yield. Since the actual rate limiting step in Suzuki cross-coupling reactions is not known, it is reasonable to make systematic adjustments to experimental variables which may affect either the oxidative addition or transmetallation step. To probe the oxidative addition step, the order of addition of the reagents was altered. The first reasonable experiment involves a "one-pot" procedure popular for Suzuki cross-coupling reactions. If this is successful, then oxidative addition would not be the rate limiting step. This reaction was attempted and resulted in an intractable mixture. Since the "one-pot" procedure was unsuccessful, sequential additions of reagents based on their order in the catalytic cycle was performed. Since the Suzuki reaction is a biphasic reaction with

organic solvent (THF) and water, the salt complex was first dissolved in water and added to the reaction mixture to avoid the possibility of salt solubility disrupting the reaction mechanism. Then, with oxidative addition being the first step, $Pd(PPh_3)_4$ in THF was added dropwise first. Postulating that this is the rate limiting step, this reaction was given some time to occur (~20 minutes), then the boronic acid substrate was added subsequently. This general procedure gave the best results. Attempts to obtain only **2-Ldm-OTf-bpA** mixtures were performed. In order to optimize this condition, the next most reasonable variable to adjust was the salt for the transmetallation step. To obtain exclusively **2-Ldm-OTf-bpA** it was believed that a weaker base could facilitate the transmetallation step. Use of a margininally weaker base, K_2CO_3 , was found to produce polymeric mixtures without any desired product. All reaction conditions resulted in polymeric mixtures in addition to the products **2-Ldm-OTf-bpA** and **3-Ldm-OTf-bpB**. However, with column chromatography techniques, these polymeric materials could be separated from **2-Ldm-OTf-bpA** and **3-Ldm-OTf-bpB**.

Variations of the Suzuki procedure were employed (including varying base, order of addition, etc.) for each reaction yielding product, starting material **1-Ldm-OTf**, **2-Ldm-OTf-bpA** and **3-Ldm-OTf-bpB** were recovered in approximately a 1:3:1 ratio or percent yield of 20% : 60% : 20%.

CONCLUSION

In summary, several novel synthons for molecular wire synthesis have been developed by manipulation of synthetic methods including Suzuki cross-coupling and aryl methyl deprotection. These new product synthons represent promising building blocks for many possible molecular wire identities and lengths for future semiconductor applications and surface functionalization of Si(111).

EXPERIMENTAL PROCEDURES

General Procedures

All reactions were performed on a Schlenk line under N_2 atmosphere, unless indicated otherwise. All solvents used were either dried over molecular sieves (4 Å) or obtained from a Pure Process Technology solvent purification system.

Physical Measurements

The ^{1}H, ^{13}C and ^{19}F NMR spectra were collected using a Bruker 400 MHz instrument; ^{1}H chemical shifts are referenced to $CDCl_3$ at 7.24 ppm for ^{1}H and 77.23 ppm for ^{13}C NMR. Some spectra contain trace solvent residues present in deuterated solvents in agreement with literature values[18].

Safety Procedures

As a strong oxidant, BBr_3 should be handled with caution and only with proper syringe technique under N_2. All quenches should be performed dropwise to a pre-chilled (0 ^{o}C) reaction flask, with time breaks upon any observation of vigorous reaction.

Synthetic Procedures

Scheme for 1L-dm-OTf

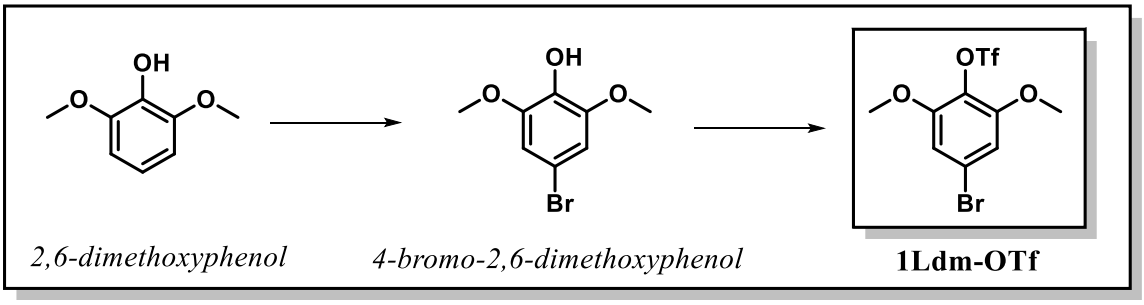

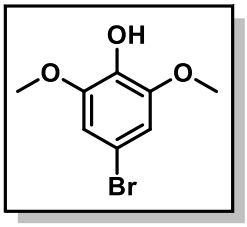

4-Bromo-2,6-dimethoxyphenol. To a dry 250 mL Schlenk flask were added 2.50 g (16.2 mmol, 1.00 equiv.) of 2,6-dimethoxyphenol and 25 mL of $CHCl_3$. The flask was chilled to –60 ^oC for 15 minutes, followed by the addition of 4.0 mg (0.16 mmol, 0.01 equiv.) of solid NaH and 2.89 g (16.2 mmol, 1.00 equiv.) of *N*-bromosuccinamide (NBS). The reaction was kept at about –40 ^oC for 3 h. After 3 h, 50 mL of deionized water was added, and the reaction was allowed to warm to room temperature. Next, 50 mL of CH_2Cl_2 was added and the solution stirred for 20 minutes. An extraction was performed and the aqueous layer was extracted with 50 mL portions of CH_2Cl_2 three times. The organic layers were collected and washed with 100 mL of 1 M $Na_2S_2O_3$. The organic

layer was washed with brine and dried over Na_2SO_4. The solution was filtered and concentrated to give a crude solid, which was purified by column chromatography on silica (100% CH_2Cl_2) to afford the product as a beige solid. Yield: 1.67 g (44%). ^{1}H NMR (400 MHz, $CDCl_3$): δ 6.72 (2H s), 5.43 (1H s), 3.87 (6H s). ^{13}C NMR (400 MHz, $CDCl_3$): δ 147.6, 134.0, 111.1, 108.5, 56.5. EIS-(+)-HRMS= *m/z* calculated for $C_8H_9BrO_3$: (^{79}Br + Na) 254.9627, (^{79}Br + Na+ H) 255.9661, (^{81}Br + Na) 256.9608, (^{81}Br + Na + H) 257.9641; found (^{79}Br + Na) 254.9621, (^{79}Br + Na+ H) 255.9657, (^{81}Br + Na) 256.9607, (^{81}Br + Na + H) 257.9635.

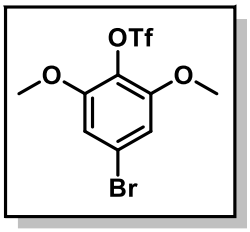

***4-Bromo-2,6-dimethoxyphenyl trifluoromethanesulfonate* (1Ldm-OTf).** To a 50 mL round bottom flask was added 1.00 g (4.29 mmol, 1.00 equiv.) of 4-bromo-2,6-dimethoxyphenol. To a separate 50 mL round bottom flask was added 1.69 g (4.72 mmol, 1.10 equiv.) of *N*-phenyl-bis(trifluoromethane sulfonamide). To another dry 250 mL Schlenk flask was added 0.170 g (7.08 mmol, 1.65 equiv.) of NaH. Subsequently, 25 mL of dry THF were added to each of the smaller round bottom flasks and 75 mL of THF were added to the Schlenk flask. Each flask was chilled on ice at 0 ^{o}C for 30 min. The solution containing 4-bromo-2,6-dimethoxyphenol was added slowly dropwise at 0 ^{o}C to the Schlenk flask containing the NaH, followed by slow dropwise addition of the *N*-phenyl-bis(trifluoromethane) sulfonamide solution at 0 ^{o}C. The reaction vessel was

allowed to warm to room temperature at stir for 30 min, after which reflux was achieved at 73 °C. After 3 h, the reaction was allowed to cool to room temperature then quenched with 30 mL of deionized water. An extraction was performed by adding 100 mL of CH_2Cl_2. The aqueous layer was then extracted three times with 100 mL of CH_2Cl_2, and the organic layers were combined. The organic phase was washed with 50 mL of H_2O, followed by 50 mL of brine, and then it was dried over Na_2SO_4. The solution was filtered and concentrated, then purified by column chromatography on silica (hexanes:CH_2Cl_2, 1:1) to afford a white solid. Yield: 1.20 g (70%). ^{1}H NMR (400 MHz, $CDCl_3$): δ 6.76 (2H s), δ 3.86 (6H s). ^{13}C NMR (400 MHz, $CDCl_3$): δ 152.9, δ 127.1, δ 120.2, δ 108.8, δ 56.6. ^{19}F NMR (400 MHz, $CDCl_3$): δ –73.61 ppm. EIS-(+)-HRMS= *m/z* calculated for $C_{43}H_{80}BrF_3O_5SSi_2$ (^{79}Br + Na) 386.9120, (^{79}Br + Na+ H) 387.9150, (^{81}Br + Na) 388.9100, (^{81}Br + Na + H) 389.9131; found (^{79}Br + Na) 386.9126, (^{79}Br + Na+ H) 387.9176, (^{81}Br + Na) 388.9100, (^{81}Br + Na + H) 389.9144.

Scheme for 1L-dSiHex$_3$-OTf

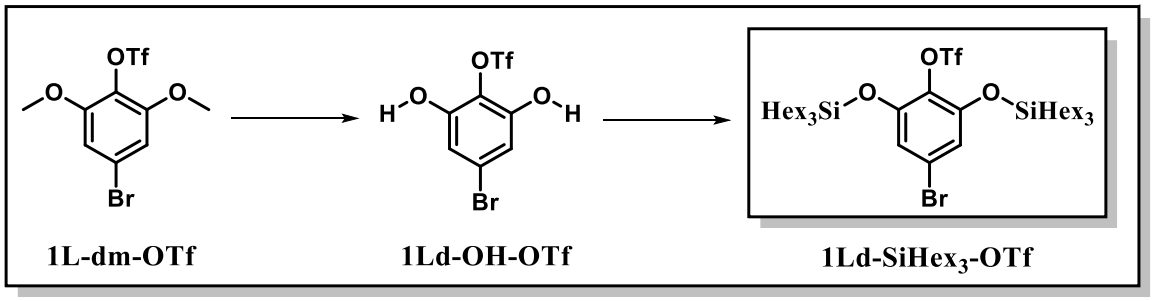

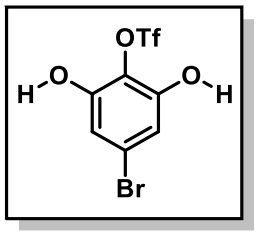

4-Bromo-2,6-dihydroxyphenyl trifluoromethanesulfonate **(1L-dOH-OTf).** To a dry round bottom flask, 0.134 g (0.368 mmol, 1.0 equiv.) of 4-bromo-2-hydroxy-6-methoxyphenyl trifluoromethanesulfonate were added, followed by 2 mL of dry CH_2Cl_2. The mixture was submerged in a dry ice/acetone bath at –75 ^oC for 20 min, then 2.05 mL (2.05 mmol, 2.50 equiv.) of BBr_3 were added. The reaction was allowed to slowly warm to room temperature and stir for 18 h overnight. An additional 2.05 mL (2.05 mmol, 2.50 equiv.) of BBr_3 was added to the flask after it had been cooled to –75 ^oC for 20 min. The reaction was allowed to slowly warm to room temperature and stir for 18 h overnight. The flask was cooled to –78 ^oC for 10 min then the reaction was quenched by a dropwise addition of 3 mL of Et_2O. The addition of Et_2O was stopped when the produced white fumes abated and the solution was no longer cloudy. Then 3 mL of sat. $NaHCO_3$ were added and ice droplets were observed in the reaction mixture at –78 ^oC. The reaction was allowed to warm to room temperature and an extraction was performed with 3 × 50 mL of CH_2Cl_2. The organic layers were collected and dried over Na_2SO_4. The crude product was purified by column chromatography on silica (EtOAc:hexanes, 1:5) to afford a white solid. Yield: 0.134 g (48%). ^1H NMR (400 MHz, $CDCl_3$): δ 6.76 (2H s), δ 5.27 (2H br s). ^{19}F NMR (400 MHz, $CDCl_3$): δ –72.92 ppm.

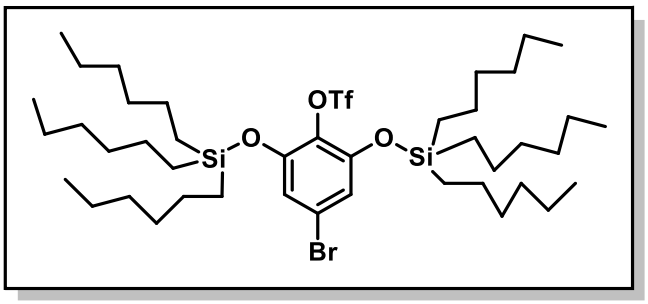

4-Bromo-2,6-bis((trihexylsilyl)oxy)phenyl trifluoromethanesulfonate **(1L-dSiHex$_3$-OTf).** To a side-arm screw-cap Schlenk flask were added 0.082 g (0.24 mmol, 1 equiv.) of **1L-dOH-OTf**. Then 1 mL of dry CH_2Cl_2 was added, followed by 0.037 g (0.54 mmol, 2.2 equiv.) of imidazole. The Schlenk flask was chilled to –20 ^oC in the fridge, followed by the dropwise addition of 0.38 g (1.20 mmol, 5.0 equiv.) of chlorotrihexylsilane. The Schlenk flask was sealed and heated to reflux at 40 ^oC overnight. The flask was cooled to room temperature and submerged in an ice bath for 10 min, then quenched with 2 mL of deionized water. The aqueous layer was extracted with CH_2Cl_2 three times in portions of 20 mL. The organic layers were collected and dried over Na_2SO_4. The solution was filtered and concentrated in vacuo. The crude product was purified by column chromatography (EtOAc:hexanes, 1:10) on silica to yield a clear oil. Yield: 0.135 g (62%). ^{1}H NMR (400 MHz, $CDCl_3$) δ 6.63 (2H s), δ 1.22 (47H m), δ 0.84 (29H m). ^{13}C NMR (400 MHz, $CDCl_3$): δ 149.83, δ 132.25, δ 120.41, δ 119.75, δ 117.62, δ 115.82, δ 33.66, δ 31.87, δ 23.48, δ 22.76, δ 16.04, δ 14.06. ^{19}F NMR (400 MHz, $CDCl_3$): δ –74.03 ppm. EIS-(+)-HRMS= *m/z* calculated for $C_{43}H_{80}BrF_3O_5SSi_2$ (^{79}Br + Na) 923.4293, (^{79}Br + Na+ H) 924.4320, (^{81}Br + Na)

925.4281, (^{81}Br + Na + H) 926.4302; found (^{79}Br + Na) 923.4271, (^{79}Br + Na+ H) 924.4306, (^{81}Br + Na) 925.4261, (^{81}Br + Na + H) 926.4289.

Scheme for 2L-dm-OTf and 3L-dm-OTf

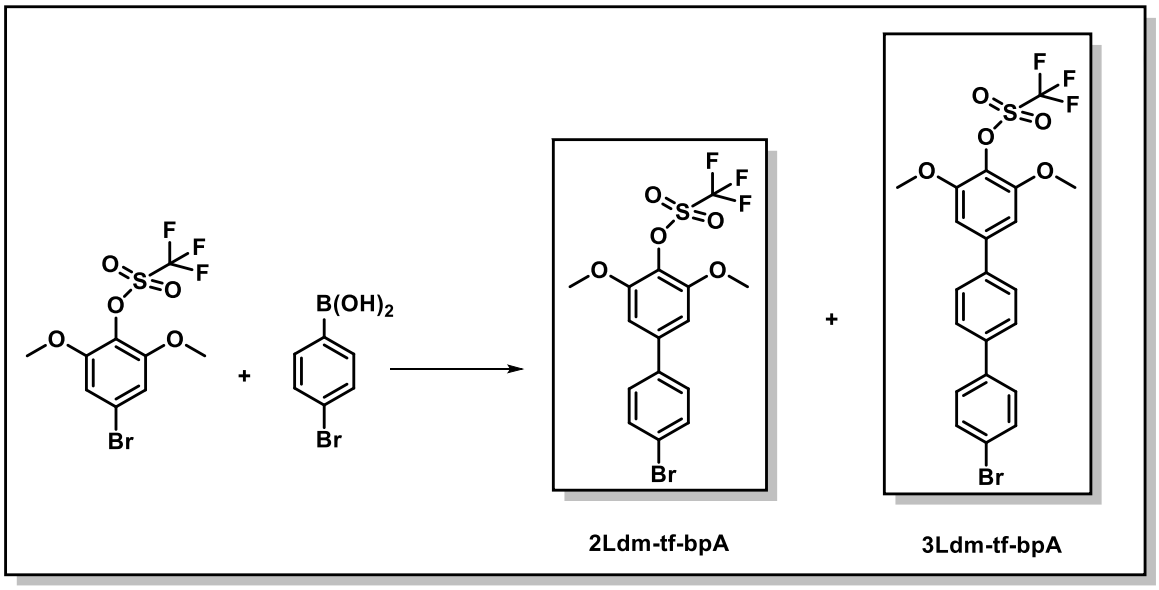

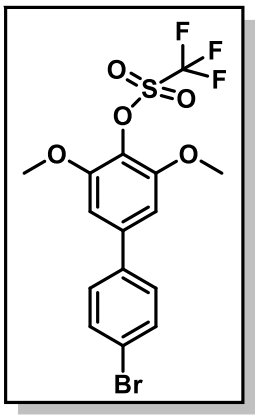

***4'-Bromo-3,5-dimethoxy-[1,1'-biphenyl]-4-yl trifluoromethanesulfonate* (2L-dm-OTf).** To a dry Schlenk flask were added 0.15 g (0.39 mmol, 1 equiv.) of **1L-dm-OTf**, which was dissolved in 2 mL of dry THF. Then 2 mL of a prepared 2 M Na_2CO_3 solution were added. In a separate vial, 0.029 g (0.039 mmol, 0.1 equiv.) of $Pd(PPh_3)_4$ was dissolved in 1 mL of dry THF. The vial was gently heated with a heat gun to generate a homogenous bright yellow solution, then allowed to cool to room temperature and the catalyst solution was added dropwise to the reaction flask. In the meantime, a vial containing 0.094 g (0.47 mmol, 1.1 equiv.) of 4-bromophenyl boronic acid under N_2 was dissolved in 1 mL of dry THF. This solution was transferred dropwise to the reaction flask. The reaction was refluxed under N_2 overnight at 73 ^oC. The reaction was allowed to cool to room temperature and placed in an ice bath for 10 min. At 0 ^oC the reaction was slowly quenched with 5 mL of deionized water. Then 5 mL of ethyl acetate were added and an extraction was performed with 3 × 20 mL of ethyl acetate. The organic layers were collected and washed with brine, then dried over Na_2SO_4. The solution was filtered and passed through a celite bed. The crude product was purified by column chromatography on silica (EtOAc:pet. ether, 5:95) to afford an amorphous off-white

material. Yield: 0.11 g (61%). ^{1}H NMR (400 MHz, $CDCl_3$) δ 7.55 (2H d), 7.40 (2H d), 6.72 (2H s), 3.93 (6H s). ^{13}C NMR (400 MHz, $CDCl_3$): δ 152.80, δ 141.32, δ 139.58, δ 132.42, δ 129.03, δ 127.81, δ 122.68, δ 122.09, δ 119.96, δ 117.83, δ 115.71, δ 104.09, δ 56.62. ^{19}F NMR (400 MHz, $CDCl_3$): δ –73.63 ppm. EIS-(+)-HRMS= *m/z* calculated for $C_{15}H_{12}BrF_3O_5S$: (^{79}Br + Na) 462.9433, (^{79}Br + Na+ H) 463.9465, (^{81}Br + Na) 464.9414, (^{81}Br + Na + H) 465.9445; found (^{79}Br + Na) 462.9431, (^{79}Br + Na+ H) 463.9473, (^{81}Br + Na) 464.9413, (^{81}Br + Na + H) 465.9431.

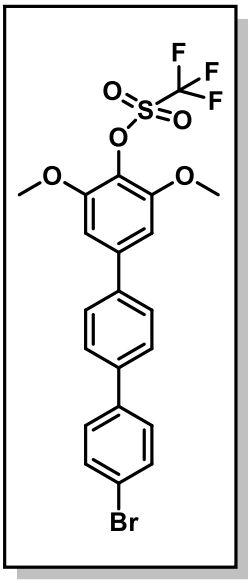

***4''-Bromo-3,5-dimethoxy-[1,1':4',1''-terphenyl]-4-yl trifluoromethanesulfonate* (3L-dm-OTf).** The compound **3L-dm-OTf** was isolated as a byproduct under the same conditions from the above reaction targeting **2L-dm-OTf**. ^{1}H NMR (400 MHz, $CDCl_3$) δ 7.60 (6H qrt), 7.48 (2H d), 6.80 (2H s), 3.94 (6H s). ^{13}C NMR (400 MHz, $CDCl_3$): δ 152.75, δ 141.87, δ 140.01, δ 139.48, δ 132.18, δ 128.92, δ 128.04, δ 127.74, δ 122.12, δ

119.98, δ 117.85, δ 115.73, δ 104.15, δ 56.65. ^{19}F NMR (400 MHz, $CDCl_3$): δ –73.63 ppm. EIS-(+)-HRMS= *m/z* calculated for $C_{21}H_{16}BrF_3O_5S$: (^{79}Br + Na) 538.9746, (^{79}Br + Na+ H) 539.9779, (^{81}Br + Na) 540.9728, (^{81}Br + Na + H) 541.9759; found (^{79}Br + Na) 538.9751, (^{79}Br + Na+ H) 539.9808, (^{81}Br + Na) 540.9726, (^{81}Br + Na + H) 541.9747.

Appendix A Supplementary Information

4-Bromo-2,6-dimethoxyphenol ^{1}H NMR

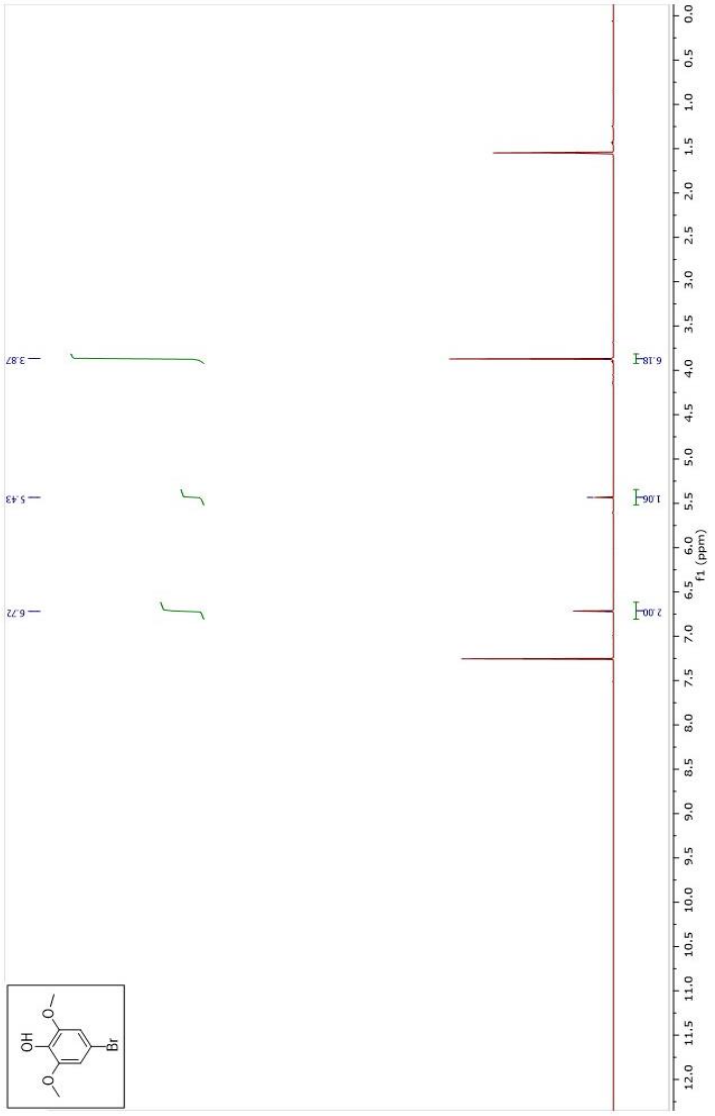

4-Bromo-2,6-dimethoxyphenol HRMS:

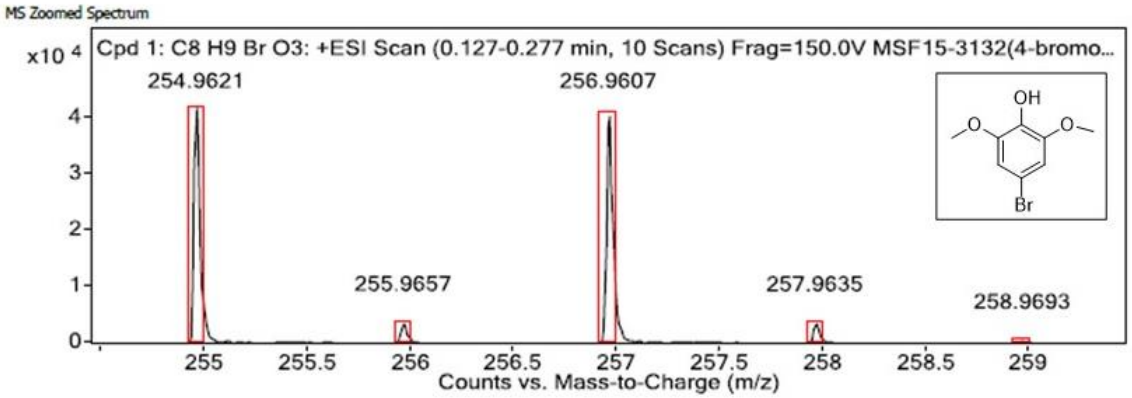

1Ldm-OTf HRMS:

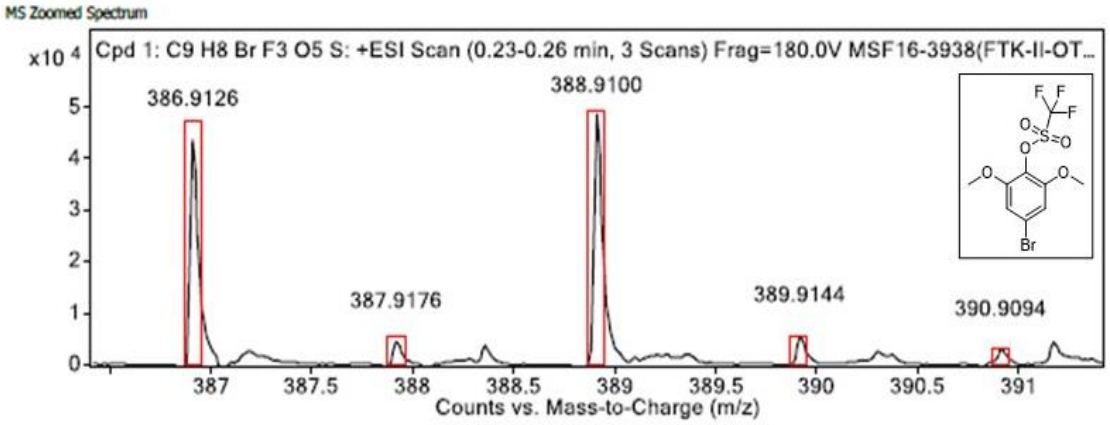

1Ldm-OTf ^{1}H NMR:

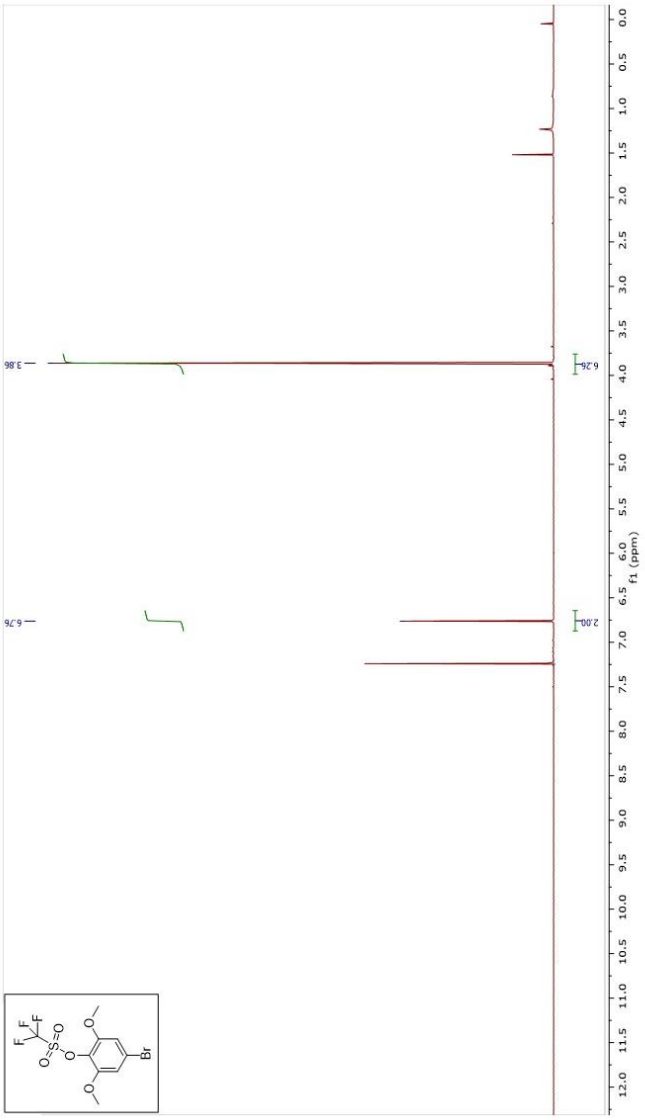

1Ldm-OTf ^{13}C NMR:

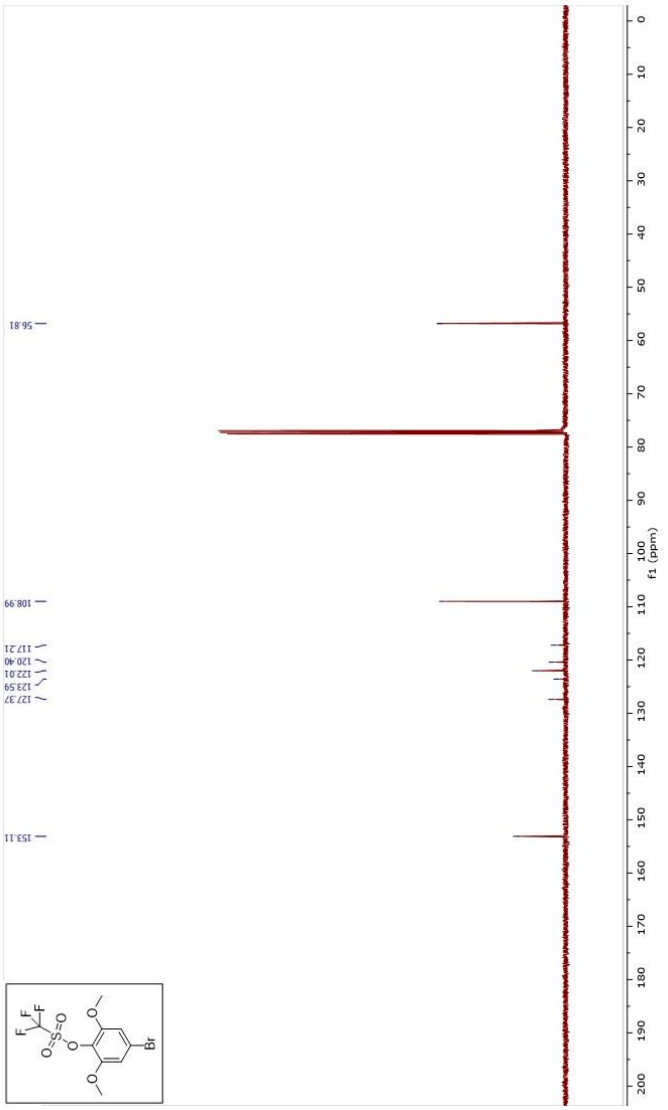

1Ldm-OTf ^{19}F NMR:

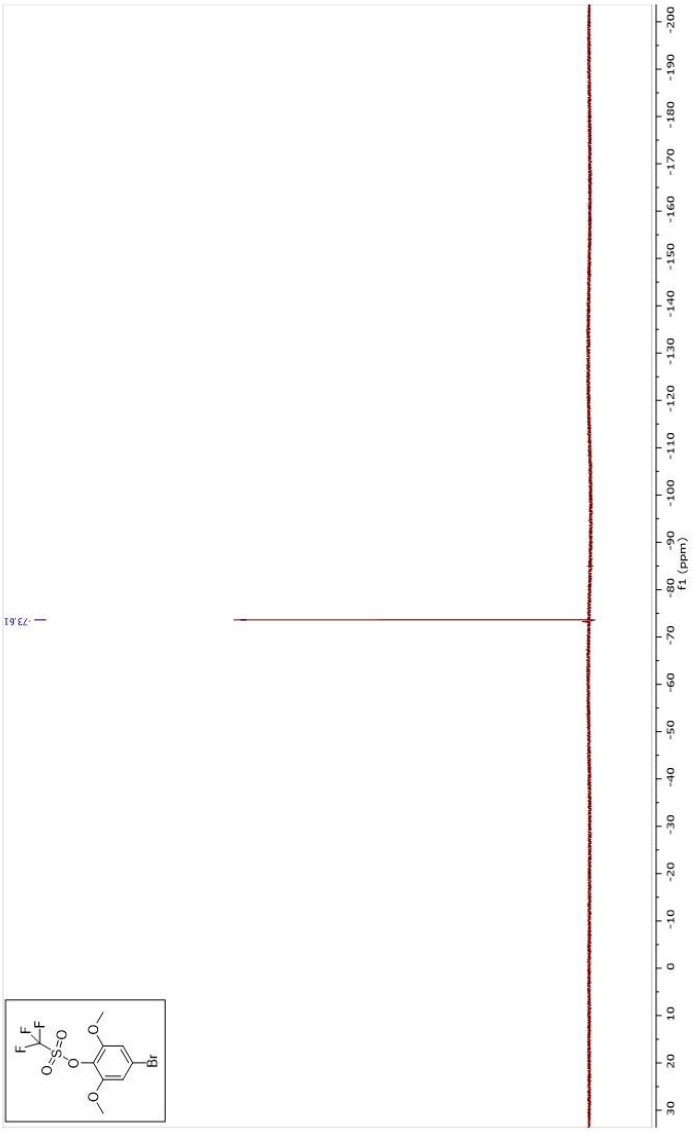

1L-dOH-OTf ^{1}H NMR:

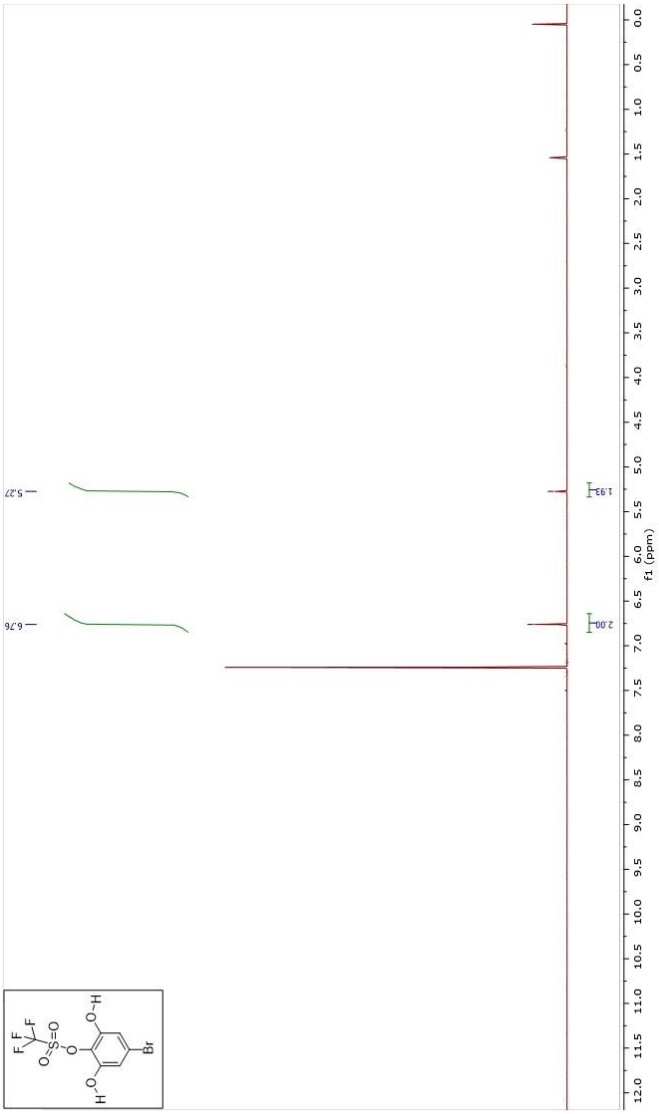

1L-dOH-OTf ^{19}F NMR:

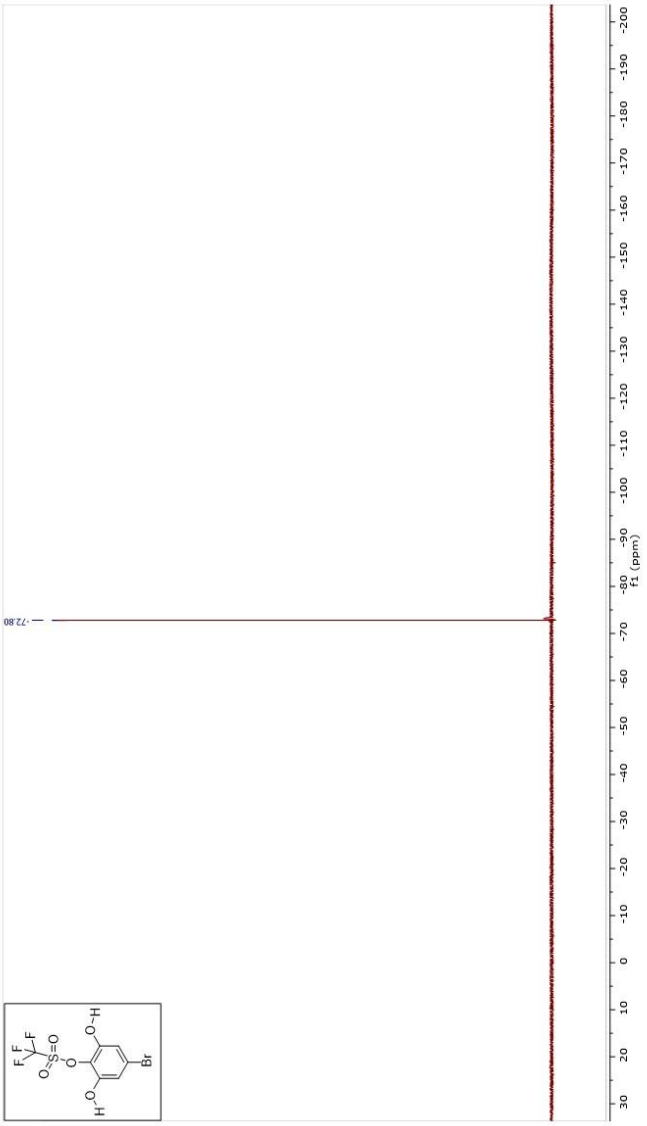

2L-dm-OTf ^{1}H NMR:

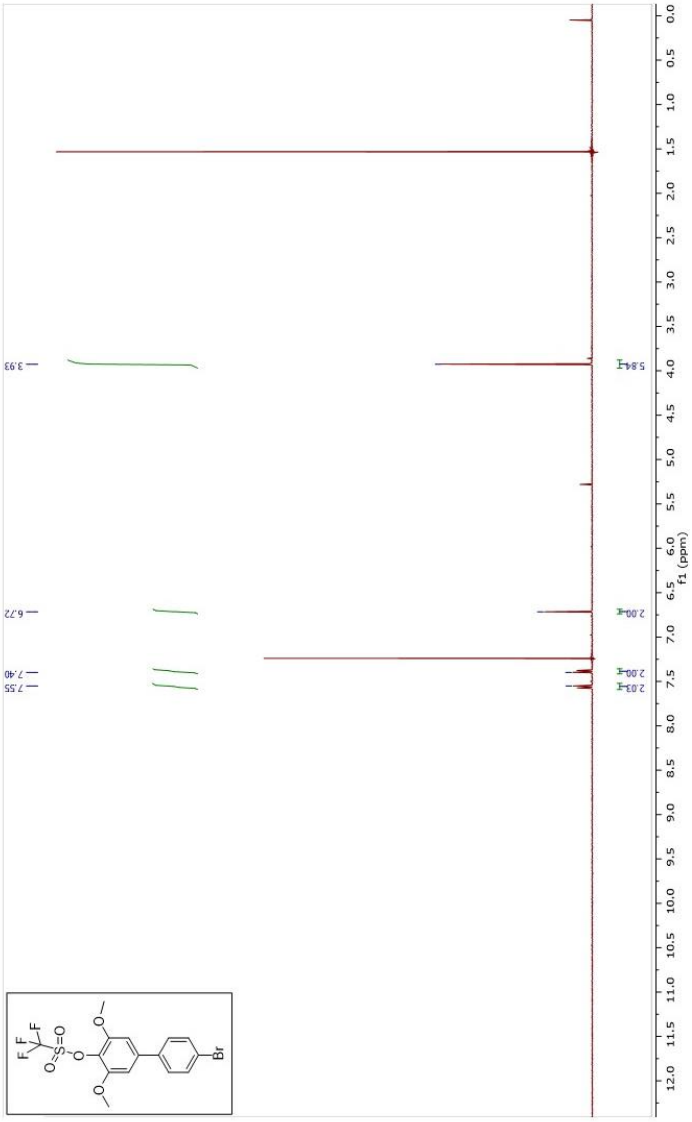

2L-dm-OTf ^{13}C NMR:

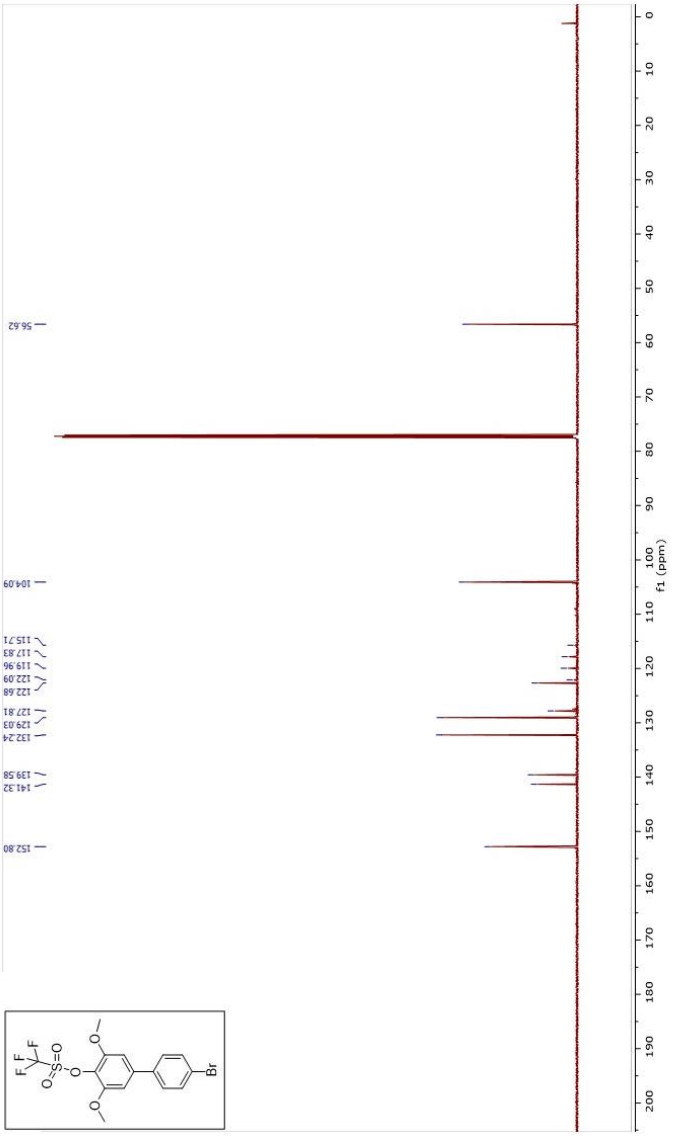

2L-dm-OTf ^{19}F NMR:

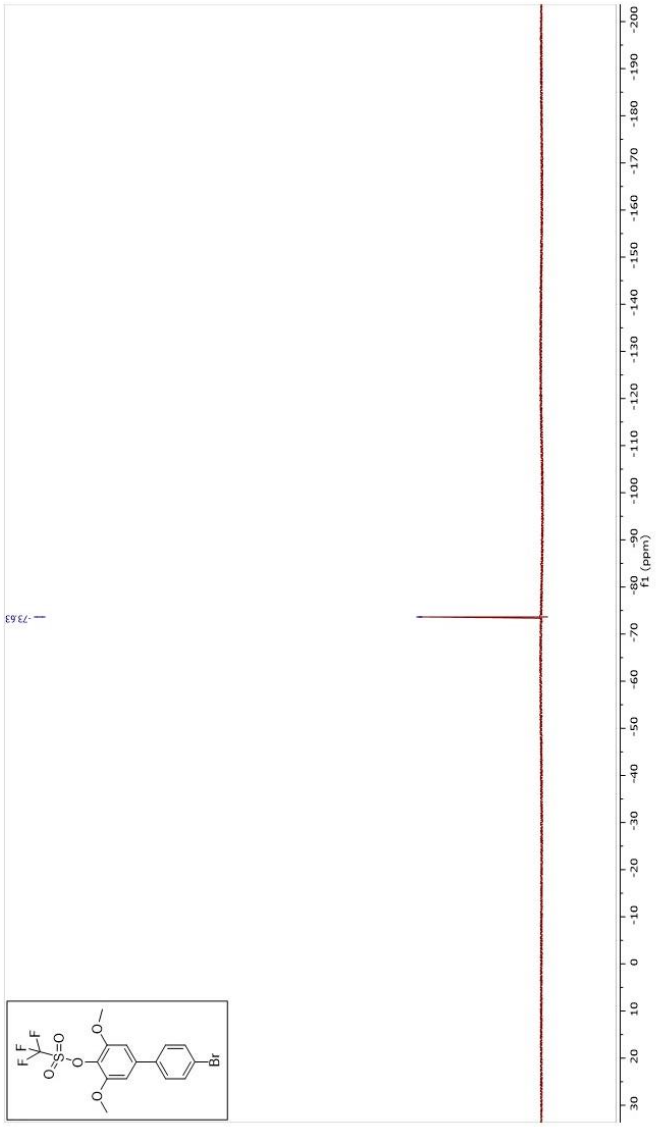

2L-dm-OTf HRMS:

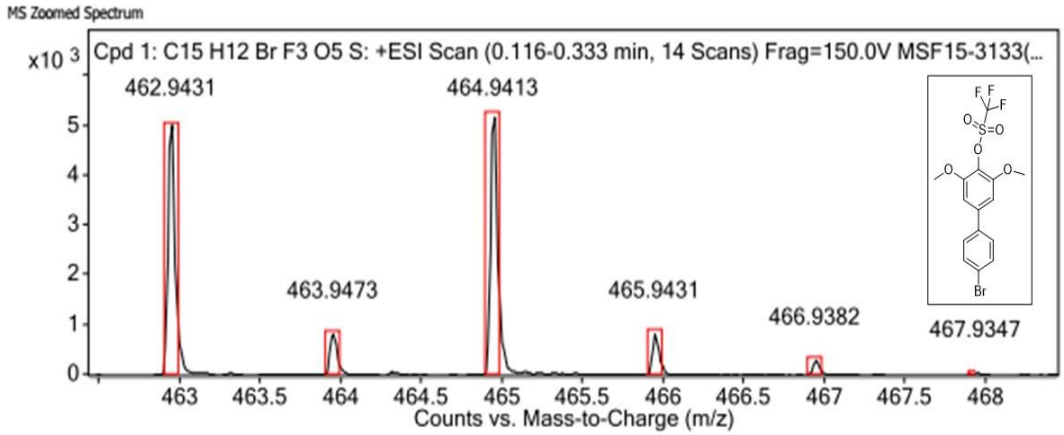

3L-dm-OTf HRMS:

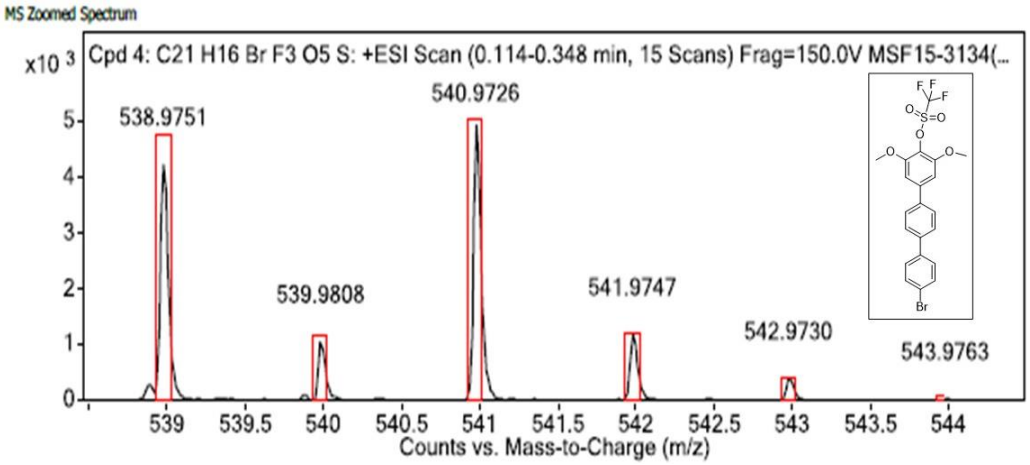

3L-dm-OTf ^{1}H NMR:

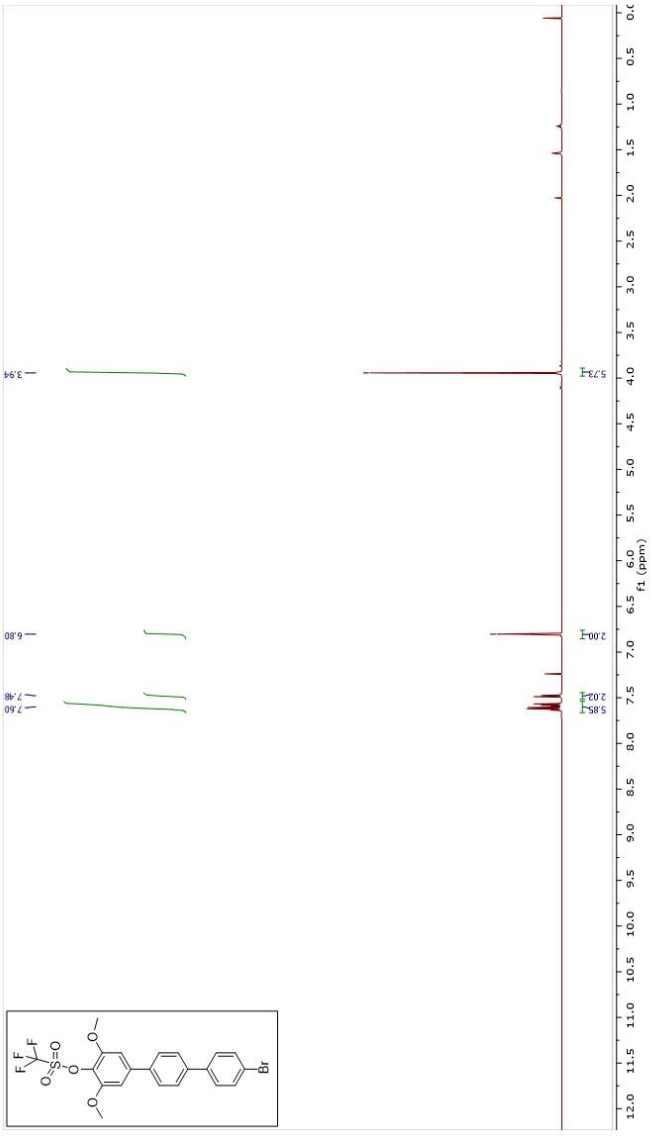

3L-dm-OTf ^{19}F NMR:

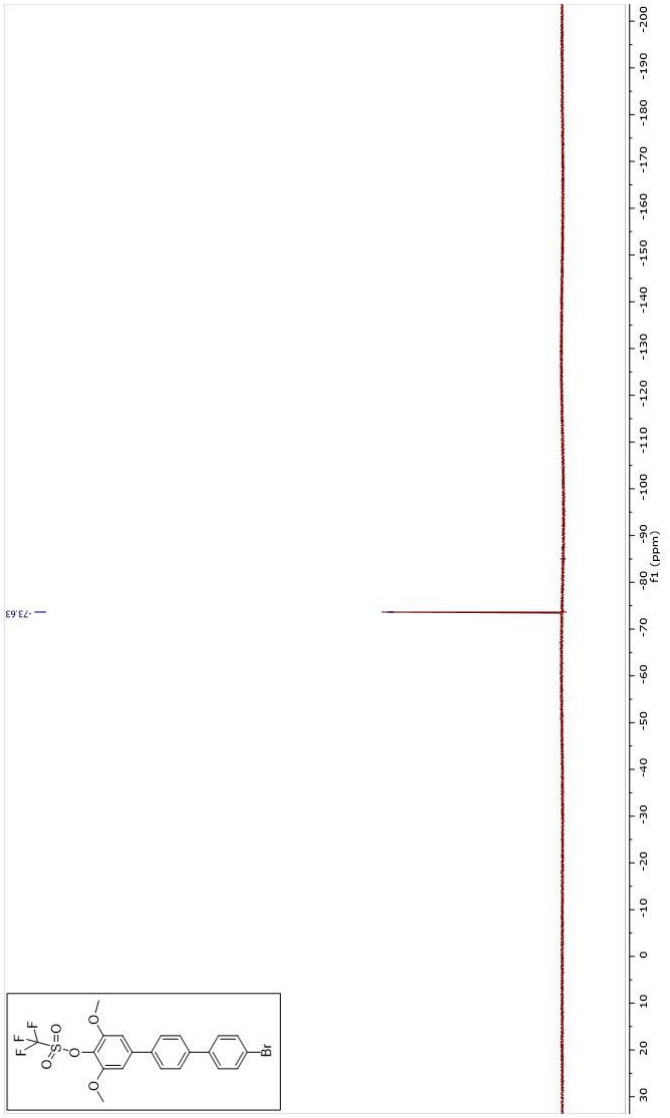

3L-dm-OTf ^{13}C NMR:

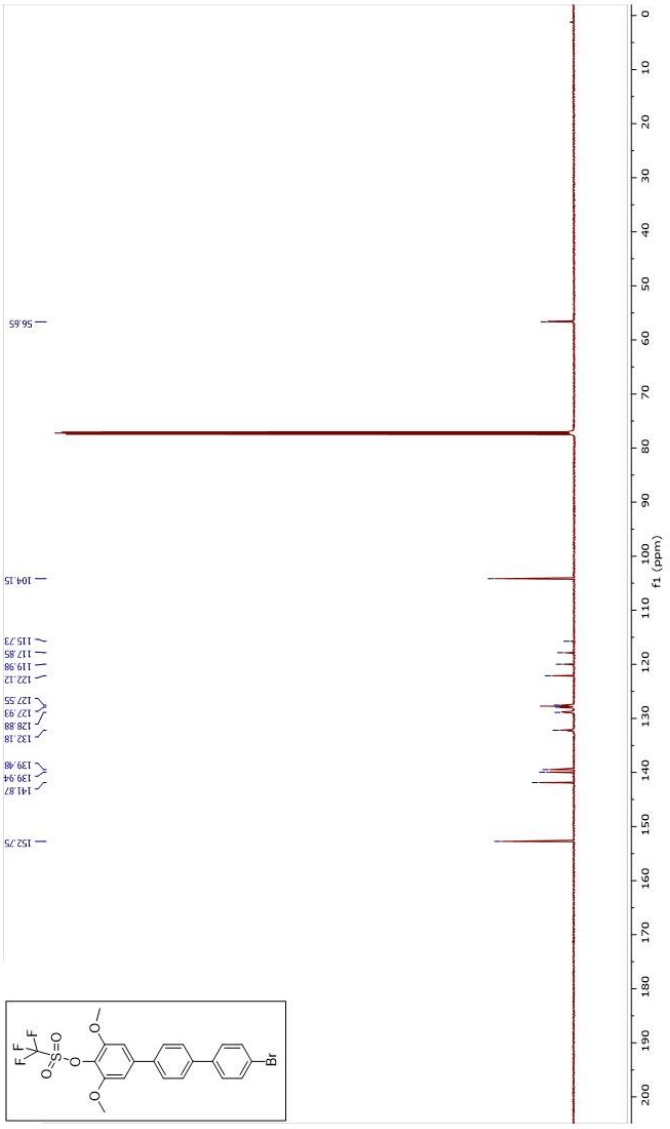

References

1) Emberly, E.; Kirczenow, G. *Nanotechnology*. **1999**, *10*, 285. "Electrical Conductance of Molecular Wires."

2) a) Vuillaume, D. *Proceedings of the IEEE.* **2010**, 1. "Molecular Nanoelectronics". b) Ratner, M. *Nat. Nanotechnol*. **2013**, *8*, 378−381. "A Brief History of Molecular Electronics."

3) a) Roth, S.; Blumentritt, S.; Burghard, M.; Cammi, E.; Carroll, D.; Curran, S.; Dusberg, G.; Liu, K.; Muster, J.; Philip, G.; Rabenau, T. *Synthetic Metals*. **1998**, *94*, 105. "Molecular Rectifiers and Transitors based on π-Conjugated Materials". b) Emberly, E.; Kirczenow. *Physical Review Letters.* **2003**, *91*, 188301. "The Smallest Molecular Switch". c) Kornyshev, A.; Kuznetsov, A.: Ulstrip, J. *PNAS.* **2006**, *103*, 6799. "In Situ Superexchange Electron Transfer Through a Single Molecule: A Rectifying Effect".

4) a) Giacomo, M.; Yue, W.; Kaner, R.; Hufaker, D. *Springer Series in Materials Science*. **2014**, *190* (High-Efficiency Solar Cells), 357. "Hybrid Solar Cells: Materials, Interfaces, and Devices." b) Vaughan, B.; Stapleton, A.; Sesa, E.; Holmes, N.; Zhou, X.; Dastoor, P.; Belcher, W. *Organic Electronics*. **2016**, *32*, 250. "Engineering Vertical Morphology with Nanoparticulate Organic Photovoltaic Devices".

5) a) Taherinia, D.; Frisbie, C. *J. Phys. Chem. C.* **2016**, *120*, 6442. "Photoswitchable Hopping Transport in Molecular Wires 4 nm in Length". b) Bredas, J.L.; Beljonne, D.; Coropceanu, V.; Cornil, J. *Chem. Rev*. **2004**, *104*, 4971. "Charge Transfer and Energy-Transfer Processes in π-Conjugated Oligomers and Polymers: A Molecular Picture." b) Ruther, R.; Cui, Q.; Hamers, R. *J. Am. Chem. Soc*. **2013**, *135*, 5751. "Conformational Disorder Enhances Electron Transfer Through Alkyl Monolayers: Ferrocene on Conductive Diamond." c) Mishchenko, A.; Vonlanthen, D.; Meded, V.; Burkle, M.; Li, C.; Pobelov, I.; Bagrets, A.: Viljas, J.; Pauly, F.; Evers, F.l Mayor, M.; Wandlowski, T. *Nano Letters*. **2010**, *10*, 156. "Influence of Conformation on Conductance of Biphenyl-Dithiol Single-Molecule Contacts". d) Su, T.; Li, H.; Steigerwald, M.; Venkataraman, L.; Nuckolls, C. *Nature Chemistry*. **2015**, *7*, 215. "Stereoelectronic Switching in Single-Molecule Junctions". e) Smith, C.; Odoh, S.; Ghosh, S.; Gagliardi, L.; Cramer, C.; Frisbie, D. *J. Am. Chem. Soc*. **2015**, *137*, 157. "Length-Dependent Nanotransport and Charge Hopping Bottlenecks in

Long Thiophene-Containing π-Conjugated Molecular Wires". f) Zhang, J.; Sun, W.; Liu, H.; He, Y.; Zhao, J. *Computational Materials Science*. **2014**, *87*, 100. "Effects of Terminal Connection and Molecular Length on Electron Transport in Linear Conjugated Molecular Wires." g) Yao, J.; Li, Y.; Zou, Z.; Wang, H.; Shen, Y. *Superlattices and Microstructures*. **2012**, *51*, 396. "First-Principles Study of the Electron Transport Through Conjugated Molecular Wires with Different Carbon Backbones." h) Nozaki, D.; Toher, C.; Cuniberti, G. *J. Phys. Chem. Lett.* **2013**, *4*, 4192. "Low-Energy Conformational Gating in π-Conjugated Molecular Junctions". i) Reecht, G.; Bulou, H.l Scheurer, F.; Speisser, V: Mathevet, F.; Gonzalez, C.; Dappe, Y.; Schull, G. *J. Phys. Chem. Lett*. **2015**, *6*, 2987. "Pulling and Stretching a Molecular Wire to Tune its Conductance". j) Lissau, H.l Frisenda, R; Olsen, S.; Jevric, M.; Parker, C.; Kadziola, A.; Hansen, T.; van der Zant, H; Nielsen, M.; Mikkelsen, K. *Nature Communications*. **2015**, *6*, 10233. "Tracking Molecular Resonance Forms of Donor-Acceptor Push-Pull Molecules By Single-Molecule Conductance Experiments".

6) Pulrey, D. *IEEE Transactions on Electronic Devices*. **1978**, *25*, 1308. "MIS Solar Cells: A Review."

7) Aviram, A; Ratner, M.A. *Chem. Phys. Lett.* **1974**, *29*, 277. "Molecular Rectifiers."

8) Ellenbogen, J.C.; Love, J.C. *Proc. IEEE*. **2000**, *88*, 386. "Architectures for Molecular Electronic Computers: 1. Logic Structures and an Adder Designed From Molecular Electronic Diodes."

9) Nakamura, H.; Asai, Y.; Hihath, J.; Bruot, C.; Tao, N. *J. Phys. Chem. C*. **2011**, *115*, 19931. "Switch of Conducting Orbital by Bias-Induced Electronic Contact Asymmetry in a Bipyrimidinyl-biphenyl Diblock Molecule: Mechanism to Achieve a pn Directional Molecular Diode".

10) Li, F.; Basile, V.; Rose, M. *Langmuir*. **2015**, *31*, 7712. "Electron Transfer through Surface Grown, Ferrocene-Capped, Oligophenylene Molecular Wires on n-Si(111) Electrodes".

11) a) Kim, H.; Kearney, K.; . Le, L.; Pekarek, R.; Rose, M.J. *ACS Appl. Mat. Intfc.* **2015**, 7, 8572. "Platinum-Enhanced Electron Transfer through Ultra-Thin Film Aluminum Oxide (Al_2O_3) on Si(111) Photoelectrodes." b) Kim, H.; Kearney, K.; Le, L.; Haber, Z.H.; Rockett, A.A.; Rose, M.J. *J. Phys. Chem. C* **2016**, 25697. "Charge-Transfer through Ultrathin Film TiO_2 on *n*-Si(111) Photoelectrodes: Experimental and Theoretical Investigation of Electric Field-Enhanced Transport with a Non-Aqueous Redox Couple."

12) Hoffmann, R.W. "Elements of Synthesis Planning." 1st Edition; Springer: Berlin Heidelberg, 2009.

13) a) Miyaura, N.; Suzuki, A. *Chem. Rev*. **1995**, *95*, 2457. "Palladium-Catalyzed Cross-Coupling Reactions of Organoboron Compounds". b) Suzuki, A. *J. of Organometallic Chemistry*. **1999**, *576*, 147. "Recent advances in the cross-coupling reactions of organoboron derivatives with organic electrophiles, 1995-1998". c) Littke, A.; Dai, C.; Fu, G. *J. Am. Chem. Soc*. **2000**, *122*, 4020. "Versatile Catalysts for the Suzuki Cross-Coupling of Arylboronic Acids with Aryl and Vinyl Halides under Mild Conditions".

14) a) Kamikawa, T.; Hayashi, T. *Tetrahedron Letters*. **1997**, *38*, 7087. "Control of Reactive Site in Palladium-Catalyzed Grignard Cross-Coupling of Arenes Containing both Bromide and Triflate". b) Furstner, A.; Leitner, A.; Mendez, M.; Krause, H. *J. Am. Chem. Soc.* **2002**, *124*, 13856. "Iron-Catalyzed Cross-Coupling Reactions".

15) Mosca, G.; Tipler, P. Physics for Scientists and Engineers: Vol 2. Electricity and Magnetism, Light, Modern Physics. 5th Edition; W.H Freeman, 2004.

16) Callister, William. Materials Science and Engineering: An Introduction. 5th edition; Wiley, 2000.

17) Ruzette, A.; Leibler, L. *Nature Materials*. **2005**, *4*, 19. "Block Copolymers in Tomorrow's Plastics".

18) Albright, T.A.; Burdett, J.K.; Whangbo, M.H. Orbital Interactions in Chemistry. Wiley Interscience; Canada, 1985.

19) Coropceanu, V.; Cornil, V.; da Silva Filho, D.; Oliver, Y.; Silbey, R.; Bredas, J.L. *Chem. Rev.* **2007**, *107*, 926. "Charge Transport in Organic Semiconductors".

20) a) Bhattarai, B.R.; Shrestha, S.; Ham, S.W; Kim, K.R.; Cheon, H.G.; Lee, K.L.; Cho, H. *Bioorganic and Medicinal Chemistry Letters*. **2007**, *19*, 5357. "2-O-Carboxymethylpyrogallol derivatives as PTP1B Inhibitors with Antihyperglycemic Activity." b) Qiu, J.; Zhao, B.; Shen, Y.; Chen, W.; Ma, Y.; Shen, Y. *European Journal of Medicinal Chemistry*. **2013**, *68*, 192. "A Novel p-terphenyl Derivative Inducing Cell-Cycle Arrest and Apoptosis in MDA-MB-435 Cells Through Topoisomerase Inhibition." c) Lalwani, K.; Sudalai, A. *European Journal of Organic Chemistry*. "First Enantioselective Synthesis of Surinamensinol B and a Non-Natural Polysporin Analogue by a Two-Stereocentered Hydrolytic Kinetic Resolution." d) Schmidt, B.; Riemer, M. *Journal of Organic Chemistry*. **2014**, *79*, 4104. "Suzuki-Miyaura Coupling of Halophenols and Phenol Boronic Acids: Systematic Investigation of Positional Isomer Effects and Conclusions for the Synthesis of Phytoalexins from Pyrinae."

21) Kosak, T.; Conrad, H.; Korich, A.; Lord, R. *Eur. J. Org. Chem.* **2015**, *34*, 7460. "Ether Cleavage Re-Investigated: Elucidating the Mechanism of BBr_3-Facilitated Demethylation of Aryl Methyl Ethers".

22) a) Yang, X.; Zhu, L.; Chen, Y.; Bao, B.; Xu, J.; Zhou, W. *Applied Surface Science*. **2016**, *376*, 1. "Controlled Hydrophilic/Hydrophobic Property of Silica Films by Manipulating the Hydrolysis and Condensation of Tetraethoxysilane". b) Weiss, F.; Topper, T.; Osmani, B.; Deyle, H.; Kovacs, G.; Mueller, B. *Langmuir*. **2016**, *32*, 3276. "Thin Film Formation and Morphology of Electrosprayed Polydimethylsiloxane".

23) a) Espino, G.; Kurbangalieva, A.; Brown, J. *Chem. Commun*. **2007**, 1742. "Aryl Bromide/Triflate Selectivities Reveal Mechanistic Divergence in Palladium-Catalyzed Couplings; The Suzuki-Miyuara Anomaly." b) Amatore, C.; Le Duc, G.; Jutand, A. *Chem. Eur. J.* 2013, 19, 10082. "Mechanism of Palladium-Catalyzed Suzuki-Miyuara Reactions: Multiple and Antagonistic Roles of Anionic "Bases" and Their Counterions".

24) Grushin, V.; Alper, H. *Chem. Rev*. **1994**, *94*, 1047. "Transformations of Chloroarenes, Catalyzed by Transition-Metal Complexes."

25) Fulmer, G.; Miller, A.; Sherden, N.; Gottlieb, H.; Nudelman, A.; Stoltz, B.; Bercaw, J.; Goldberg, K. *Organometallics.* **2010**, *29*, 2176. "NMR Chemical Shifts of Trace Impurities: Common Laboratory Solvents, Organics, and Gases in Deuterated Solvents Relevant to the Organometallic Chemist".

26) a) Bhattarai, B.R.; Shrestha, S.; Ham, S.W; Kim, K.R.; Cheon, H.G.; Lee, K.L.; Cho, H. *Bioorganic and Medicinal Chemistry Letters*. **2007**, *19*, 5357. "2-O-Carboxymethylpyrogallol derivatives as PTP1B Inhibitors with Antihyperglycemic Activity." b) Qiu, J.; Zhao, B.; Shen, Y.; Chen, W.; Ma, Y.; Shen, Y. *European Journal of Medicinal Chemistry*. **2013**, *68*, 192. "A Novel p-terphenyl Derivative Inducing Cell-Cycle Arrest and Apoptosis in MDA-MB-435 Cells Through Topoisomerase Inhibition." c) Lalwani, K.; Sudalai, A. *European Journal of Organic Chemistry*. **2015**, *33*, 7344. "First Enantioselective Synthesis of Surinamensinol B and a Non-Natural Polysporin Analogue by a Two-Stereocentered Hydrolytic Kinetic Resolution." d) Schmidt, B.; Riemer, M. *Journal of Organic Chemistry*. **2014**, *79*, 4104. "Suzuki-Miyaura Coupling of Halophenols and Phenol Boronic Acids: Systematic Investigation of Positional Isomer Effects and Conclusions for the Synthesis of Phytoalexins from Pyrinae."